CANCER

# The kinase activity of the Ser/Thr kinase BUB1 promotes TGF-β signaling

Shyam Nyati,[1,2] Katrina Schinske-Sebolt,[2] Sethuramasundaram Pitchiaya,[3,4] Katerina Chekhovskiy,[2] Areeb Chator,[2] Nauman Chaudhry,[2] Joseph Dosch,[5] Marcian E. Van Dort,[5] Sooryanarayana Varambally,[6] Chandan Kumar-Sinha,[6,7] Mukesh Kumar Nyati,[2] Dipankar Ray,[2] Nils G. Walter,[3,4] Hongtao Yu,[8,9] Brian Dale Ross,[1,5] Alnawaz Rehemtulla[1,2]*

**Transforming growth factor–β (TGF-β) signaling regulates cell proliferation and differentiation, which contributes to development and disease. Upon binding TGF-β, the type I receptor (TGFBRI) binds TGFBRII, leading to the activation of the transcription factors SMAD2 and SMAD3. Using an RNA interference screen of the human kinome and a live-cell reporter for TGFBR activity, we identified the kinase BUB1 (budding uninhibited by benzimidazoles-1) as a key mediator of TGF-β signaling. BUB1 interacted with TGFBRI in the presence of TGF-β and promoted the heterodimerization of TGFBRI and TGFBRII. Additionally, BUB1 interacted with TGFBRII, suggesting the formation of a ternary complex. Knocking down BUB1 prevented the recruitment of SMAD3 to the receptor complex, the phosphorylation of SMAD2 and SMAD3 and their interaction with SMAD4, SMAD-dependent transcription, and TGF-β–mediated changes in cellular phenotype including epithelial-mesenchymal transition (EMT), migration, and invasion. Knockdown of BUB1 also impaired noncanonical TGF-β signaling mediated by the kinases AKT and p38 MAPK (mitogen-activated protein kinase). The ability of BUB1 to promote TGF-β signaling depended on the kinase activity of BUB1. A small-molecule inhibitor of the kinase activity of BUB1 (2OH-BNPP1) and a kinase-deficient mutant of BUB1 suppressed TGF-β signaling and formation of the ternary complex in various normal and cancer cell lines. 2OH-BNPP1 administration to mice bearing lung carcinoma xenografts reduced the amount of phosphorylated SMAD2 in tumor tissue. These findings indicated that BUB1 functions as a kinase in the TGF-β pathway in a role beyond its established function in cell cycle regulation and chromosome cohesion.**

## INTRODUCTION

The transforming growth factor–β (TGF-β) family of cytokines regulates many processes such as immune suppression, angiogenesis, wound healing, and epithelial-mesenchymal transition (EMT) (*1*, *2*). Abnormal TGF-β signaling is linked to autoimmune and inflammatory diseases, fibrosis, tumor formation and metastasis, and various other disorders. Early in tumorigenesis, the proliferation of epithelial cells retains exquisite sensitivity to TGF-β, wherein TGF-β elicits a tumor-suppressive response. However, transformed cells become refractory to TGF-β–mediated growth inhibition and acquire a phenotype wherein the intracellular signaling circuitry is altered, leading to tumorigenic and metastatic effects in response to TGF-β (*3*). These responses are diverse, depending on signaling from growth factor receptors activated in parallel (*4*), cell density and cell cycle phase (*5*), and the abundance and activity of transcriptional regulators (*6*).

BUB1 (budding uninhibited by benzimidazoles-1) is a serine/threonine kinase that is encoded by the *BUB1* gene [40 kilo–base pairs (kbp), 25 exons] in humans. During mitosis, BUB1 binds kinetochores and plays a key role in establishing the mitotic spindle checkpoint and aligning chromosomes (*7*), in addition to its central role in ensuring fidelity during chromosomal segregation into daughter cells (*8*). Three main regions have been identified in BUB1: a conserved N-terminal region that contains the kinetochore localization domain; an intermediate, nonconserved region that is required as a scaffold for the recruitment of proteins; and a C-terminal region that contains a catalytic serine/threonine kinase domain (*9*). Mutations in *BUB1* are associated with aneuploidy and several types of cancer.

Ligand-dependent activation of TGF-β receptors and regulation of their subsequent kinase activity is a complex process that can involve several posttranslational modifications of the receptors [including autophosphorylation (*10*), cross-phosphorylation (*11*), trans-phosphorylation (*12*), ubiquitylation (*13*), sumoylation (*14*), and dephosphorylation (*15*)], as well as internalization of the receptor-ligand complex (*16*–*19*). With so much complexity in one pathway, we set out to find potentially new regulators of TGF-β receptor activity.

## RESULTS

### Kinase-targeted high-throughput small interfering RNA screen identifies regulators of TGF-β signaling

To identify proteins that regulate signaling by the type I TGF-β receptor (TGFBRI), we transfected small interfering RNAs (siRNAs) against each of the 720 known and predicted kinases into A549 lung adenocarcinoma and MDA-231-1833 breast cancer cells that stably expressed a reporter for TGFBRI kinase activity [(BTR (*4*)] and screened for an increase in bioluminescence after the addition of TGF-β ligand to the culture

[1]Center for Molecular Imaging, University of Michigan, Ann Arbor, MI 48109, USA. [2]Department of Radiation Oncology, University of Michigan, Ann Arbor, MI 48109, USA. [3]Single Molecule Analysis in Real-Time (SMART) Center, University of Michigan, Ann Arbor, MI 48109, USA. [4]Department of Chemistry, University of Michigan, Ann Arbor, MI 48109, USA. [5]Department of Radiology, University of Michigan, Ann Arbor, MI 48109, USA. [6]Department of Pathology, University of Michigan, Ann Arbor, MI 48109, USA. [7]Michigan Center for Translational Pathology, University of Michigan, Ann Arbor, MI 48109, USA. [8]Howard Hughes Medical Institute, University of Texas Southwestern Medical Center, Dallas, TX 75390, USA. [9]Department of Pharmacology, University of Texas Southwestern Medical Center, Dallas, TX 75390, USA.
*Corresponding author. E-mail: alnawaz@med.umich.edu

Downloaded from http://stke.sciencemag.org/ on January 8, 2015

medium (fig. S1A). BTR is a reporter that exhibits increased luminescence upon loss of TGFBRI kinase activity; thus, positive hits from the siRNA screen identify genes that encode proteins that promote TGFBRI kinase activity. We used a quartile-based method to identify proteins that, when knocked down, induced more than 7.14-fold activation of the reporter in A549 cells and more than 13.91-fold in MDA-231-1833 cells (high-stringency hits, targeted error rate $\alpha = 0.0027$), followed by experiment- and plate-wise analysis of the normalized fold induction (Fig. 1, A to C, and table S1) as previously described (*20*). Eight hits were identified in A549-BTR cells (Fig. 1A), whereas 15 were recovered in MDA-231-1833–BTR cells (Fig. 1B). Two of these hits were the kinases BMPR2 (in A549-BTR cells) and RPS6KB1 (in MDA-231-1833–BTR cells), which are already associated with the TGF-β pathway (table S2). Analysis at a lower stringency (5.4-fold in A549 cells, 10.29-fold in MDA-231-1833 cells, targeted error rate $\alpha = 0.046$) revealed additional hits, several of which also have known roles in regulating TGF-β signaling (table S2), thereby further validating the screen.

A logical relations analysis of the A549-BTR and MDA-231-1833–BTR screens revealed that a large majority of the significant hits were distinct for each cell line (Fig. 1C); of these, seven were common (Fig. 1C). Signaling pathway impact analysis demonstrated that signaling networks previously implicated in promoting the cellular response to TGF-β [including those mediated by receptor tyrosine kinases (RTKs), mitogen-activated protein kinase (MAPK), and phosphoinositide 3-kinase (PI3K)–AKT] were identified as hits in the screen (table S3 and fig. S1, B and C) (*4*). Targets within the progesterone-mediated oocyte maturation and the oocyte meiosis pathways, in which BUB1 is a key component, consistently exhibited high perturbation accumulation in A549-BTR and MDA-231-1833–BTR cells (fig. S1, B and C).

## BUB1 promotes canonical and noncanonical TGF-β signaling

In an effort to biochemically validate these findings, we knocked down select hits in MRC5 (human fetal lung fibroblast), Het1A (human esophageal epithelial), A549-BTR (lung adenocarcinoma), MDA-231-1833–BTR (breast cancer), MCF7 (breast cancer), and MCF10A (human mammary epithelial) cells. BUB1 knockdown induced the most robust decrease in TGF-β–dependent SMAD2 phosphorylation (fig. S2) and was selected for further study. Similar to a positive control, in which TGFBRI was silenced, knockdown of BUB1 in lung cancer (A549 and NCI-H358) and breast cancer (MDA-231-1833) cell lines using siRNAs abrogated the activation of SMAD2 and SMAD3, as well as components of the noncanonical signaling cascade (c-JUN, p38 MAPK, and AKT) in each of the cell lines (Fig. 1D), key downstream effectors of TGF-β signaling (*21*, *22*). Transfection with BUB1 siRNA caused a similar decrease in TGFBRI abundance as did TGFBRI siRNA, but only in A549 cells. Even still, in this cell line, the effects of BUB1 siRNA did not mimic the effects of TGFBRI siRNA. Thus, the effects of BUB1 knockdown on downstream markers of TGF-β signaling were not an artifact of off-target or indirect knockdown of TGFBRI.

## BUB1 mediates TGF-β–dependent recruitment of R-SMADs to the activated receptor

Because depletion of BUB1 reduced TGF-β–mediated SMAD2/3 phosphorylation, we hypothesized that BUB1 may mediate the efficient recruitment of SMAD2/3 to the activated receptor in the presence of ligand. To test this hypothesis, A549 and human embryonic kidney (HEK) 293T cells were transfected with Flag-tagged SMAD3 and His-tagged TGFBRI in the presence of control or TGFBRI- or BUB1-targeted siRNA and subsequently treated with TGF-β for 1 hour. Coimmunoprecipitation analysis revealed that either TGFBRI or BUB1 knockdown impaired SMAD3 binding to TGFBRI in the presence of ligand (Fig. 2, A and B, and fig. S3, A to C).

Upon phosphorylation, receptor-regulated SMADs (R-SMADs, including SMADs 1, 2, 3, 5, and 8/9) translocate to the nucleus, wherein they regulate transcription of specific target genes. We evaluated the effect of BUB1 knockdown on the nuclear translocation of SMAD2 as a surrogate for the activation of the TGF-β pathway by immunofluorescence microscopy. A549 and H358 cells were transfected with control or TGFBRI- or BUB1-targeted siRNA stimulated with TGF-β for 1 hour. In control cells, SMAD2 was predominantly localized to the nucleus upon TGF-β stimulation; in contrast, in cells depleted of either TGFBRI or BUB1, SMAD2 translocation to the nucleus was similarly impaired (fig. S3D). Together, these results suggest that BUB1 plays an important role in promoting canonical and noncanonical TGF-β signaling.

## BUB1 promotes R-SMAD/SMAD4 complex formation and target gene transcription

To extend our finding that depletion of BUB1 leads to reduced R-SMAD recruitment to the receptor complex and hence reduced phosphorylation and nuclear translocation, we investigated whether BUB1 also promotes SMAD2/3-SMAD4 complex formation using coimmunoprecipitation assays. As expected, depletion of TGFBRI in A549 cells impaired TGF-β–induced formation of a SMAD2/3-SMAD4 complex (Fig. 2C and fig. S4). To evaluate a role for BUB1 in TGF-β–induced gene expression, we used the SBE4-Luc reporter (*6*). In A549 cells transfected with control siRNA, TGF-β induced a time-dependent increase in reporter activity, but this induction was abrogated by depletion of BUB1 (Fig. 2, D and E). Similar observations were seen in lung (NCI-H358), breast (MDA-231-1833), and cervical (HeLa) cancer cell lines (Fig. 2, F to H).

One of the expression signatures induced by TGF-β signaling is that which promotes EMT, a process in epithelial cells that occurs during development and disease progression in response to specific stimuli (*23*). Addition of TGF-β to epithelial cells in culture induces features of EMT, including the adoption of a spindle-like mesenchymal morphology and invasive behavior (*24*–*26*). Therefore, we investigated the role of BUB1 in TGF-β–mediated EMT. As expected, cultures of A549 or NCI-H358 cells exhibited a transition to a mesenchymal phenotype in response to TGF-β; however, TGFBRI or BUB1 knockdown prevented this transition (fig. S5, A to E). Similar to the effect of silencing TGFBRI, knocking down BUB1 significantly inhibited TGF-β–mediated induction of cell migration and invasion in culture (fig. S6, A to D). These results further support a role for BUB1 in mediating TGF-β signaling.

## Catalytic activity is required for BUB1 to mediate TGF-β signaling

To confirm that the kinase activity of BUB1 mediated TGF-β signaling, we conducted rescue experiments in A549 cells using siRNA-resistant constructs of BUB1 (*27*). In cells depleted of endogenous BUB1, restoration with wild-type BUB1, but not a kinase-deficient BUB1 mutant, rescued SMAD2/3 phosphorylation in a ligand-dependent manner (Fig. 3A and fig. S7A). In agreement with this observation, reporter activity in BUB1-depleted A549 cells expressing the SBE4-Luc promoter was restored upon expression of wild-type, but not a kinase-deficient, BUB1 (Fig. 3B), demonstrating a requirement for BUB1's kinase activity in its role in TGF-β signaling. The concentration of 2OH-BNPP, a catalytic BUB1 inhibitor (*9*), negatively correlated with the phosphorylation of SMAD2 and SMAD3 (fig. S7, B to D). Blocking the activity of BUB1 with 2OH-BNPP1 dose-dependently impaired the TGF-β–induced phosphorylation of proteins that mediate canonical and noncanonical TGF-β signaling in

Downloaded from http://stke.sciencemag.org/ on January 8, 2015

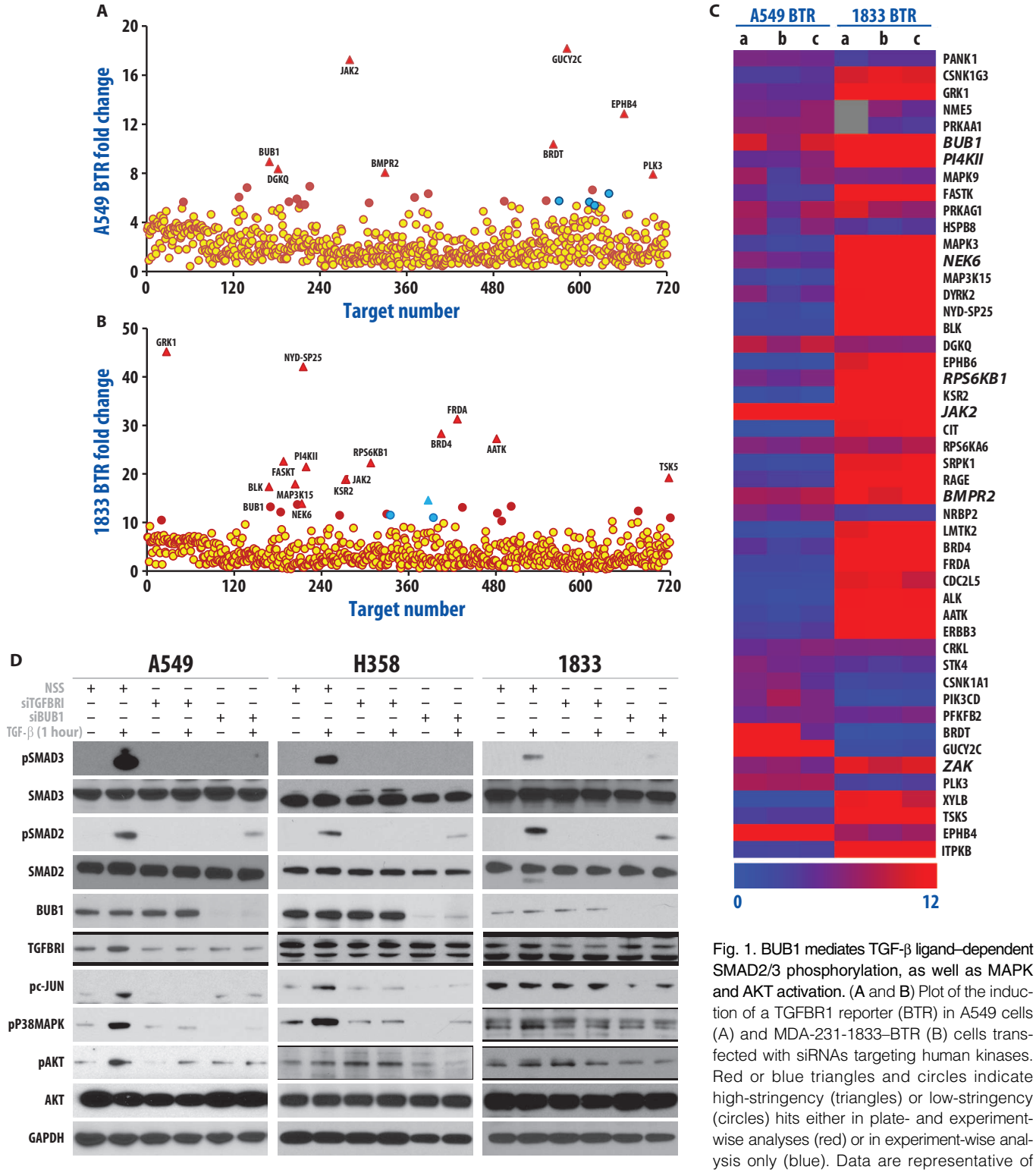


Fig. 1. BUB1 mediates TGF-β ligand–dependent SMAD2/3 phosphorylation, as well as MAPK and AKT activation. (A and B) Plot of the induction of a TGFBR1 reporter (BTR) in A549 cells (A) and MDA-231-1833–BTR (B) cells transfected with siRNAs targeting human kinases. Red or blue triangles and circles indicate high-stringency (triangles) or low-stringency (circles) hits either in plate- and experiment-wise analyses (red) or in experiment-wise analysis only (blue). Data are representative of three independent experiments. (C) Heat map of low-stringency hits in A549-BTR and MDA-231-1833–BTR cells from triplicate experiments. Gene name in italics indicates common hits. (D) Western blot analysis of TGF-β effector molecules in A549, NCI-H358, and MDA-231-1833 cells transfected with siRNA against either BUB1 (siBUB1) or TGFBRI (siTGFBRI) or a scrambled control siRNA [nonsilencing siRNA (NSS)] in the presence of TGF-β ligand for 1 hour. Blots are representative of three independent experiments.

Downloaded from http://stke.sciencemag.org/ on January 8, 2015

multiple cancer cell lines (Fig. 3, C to E) and normal cell lines (fig. S7, E and F). Similar to the effects of a pharmacological TGFBRI inhibitor [SB431542 (*28*)], 2OH-BNPP impaired the nuclear translocation of SMAD2 (fig. S7, G and H), SMAD2/3-SMAD4 complex formation (Fig. 3, F and G), and SBE4-Luc reporter activity (Fig. 3, H and I, and fig. S7, I and J) in response to TGF-β in various cell lines.

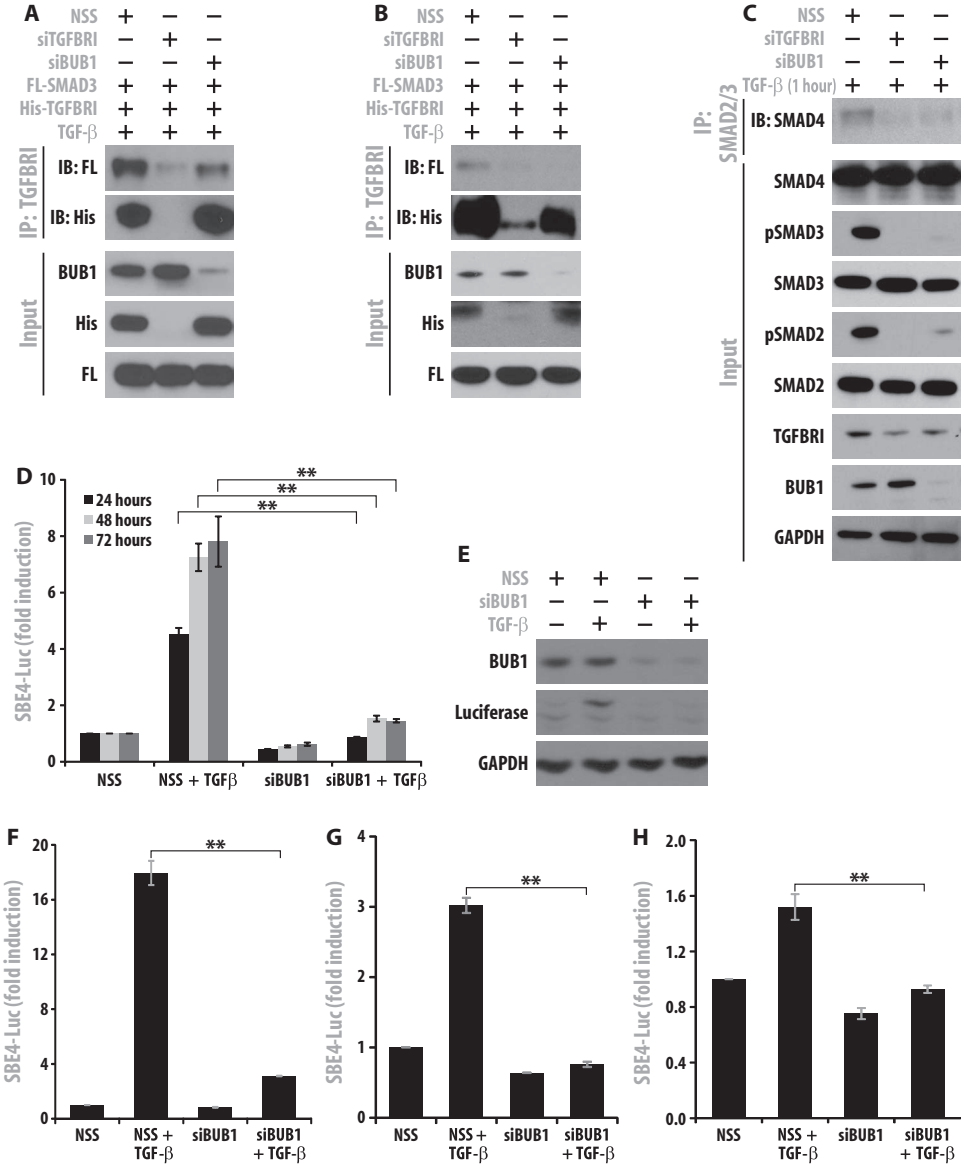


Fig. 2. BUB1 promotes the recruitment of SMAD3 to TGFBRI, SMAD2/3-SMAD4 complex formation, and transcriptional response. (**A** and **B**) Immunoprecipitation (IP) for the TGFBRI antibody and then immunoblotting (IB) for the Flag or His tags in HEK293T (A) and A549 (B) cells transfected with control siRNA (NSS), TGFBRI siRNA, or BUB1 siRNA along with Flag-tagged SMAD3 (FL-SMAD3) and 6XHis-tagged TGFBRI (His-TGFBRI) and treated with TGF-β (1 hour). (**C**) IP for SMAD2/3 followed by blotting for SMAD4 in lysates from A549 cells transfected with control siRNA, TGFBR1 siRNA, or BUB1 siRNA and treated with TGF-β (1 hour). (**D**) Relative firefly luciferase activity (normalized to Gaussia luciferase) after addition of TGF-β (10 ng/ml) and transfection with mock (NSS) or BUB1 siRNA for 24 to 72 hours in A549 cells transiently transfected with an SBE4-Luc reporter and GLuc plasmids. (**E**) Immunoblotting for luciferase and BUB1 in lysates from A549 cells transfected and treated as in (D) and harvested 24 hours after TGF-β treatment. (**F** to **H**) Relative luciferase activity in NCI-H358 (F), MDA-231-1833 (G), and HeLa (H) transfected as in (D) and treated with TGF-β (10 ng/ml) for 24 hours. Blots are representative of three independent experiments. Data are means ± SEM of three independent experiments. $^{**}P < 0.001$, two-sided Student's *t* test.

## BUB1 colocalizes and interacts with TGFBRI in response to TGF-β stimulation

On the basis of the observed role of BUB1 in promoting the recruitment of SMAD3 to TGFBRI (Fig. 2, A and B, and fig. S3, A and B) and previous evidence of a scaffolding function for BUB1 (*7*–*9*, *29*), we investigated whether BUB1 physically interacts with TGFBRI to mediate its activity using total internal reflection fluorescence (TIRF) microscopy (*30*). TIRF images revealed the presence of BUB1 and TGFBRI in punctate structures within the plasma membrane plane (Fig. 4A). Spectral analysis detected negligible colocalization of TGFBRI and BUB1 at 1 and 24 hours after ligand stimulation (fig. S8A), possibly because of the signal from the relatively high abundance of cytoplasmic BUB1. In contrast, by 72 hours with TGF-β, the proportion of colocalized TGFBRI and BUB1 signals doubled (Fig. 4, A to C).

We next examined whether forced overexpression of BUB1 using a Myc-tagged construct was sufficient for its interaction with TGFBRI, and if this would affect the phosphorylation of SMAD2/3. Heterologous expression of BUB1 in A549 cells resulted in the coimmunoprecipitation of BUB1 and TGFBRI regardless of TGF-β ligand (Fig. 4D and fig. S8B), but this was not sufficient to initiate SMAD2/3 phosphorylation in the absence of ligand, only modestly increased phosphorylation of SMAD3 (but not SMAD2) in the presence of TGF-β (Fig. 4D and fig. S8C). Overexpression of both BUB1 and TGFBRI induced a markedly greater TGF-β–stimulated interaction between BUB1 and TGFBRI and further increased the phosphorylation of SMAD3 (Fig. 4D and fig. S8, B and C). These results demonstrate that overexpression of TGFBRI and/or BUB1 enhances the activation of the signaling pathway only in the presence of the TGF-β ligand. Myc-tagged BUB1 coimmunoprecipitated with a His-tagged cytoplasmic tail of TGFBRI from A549 cell lysates (Fig. 4E), demonstrating that BUB1 may interact with the cytoplasmic tail of TGFBRI.

## BUB1 mediates TGF-β–dependent TGFBRI-TGFBRII heteromeric complex formation

In the presence of ligand, TGFBRI is recruited to the type II receptor (TGFBRII)

Downloaded from http://stke.sciencemag.org/ on January 8, 2015

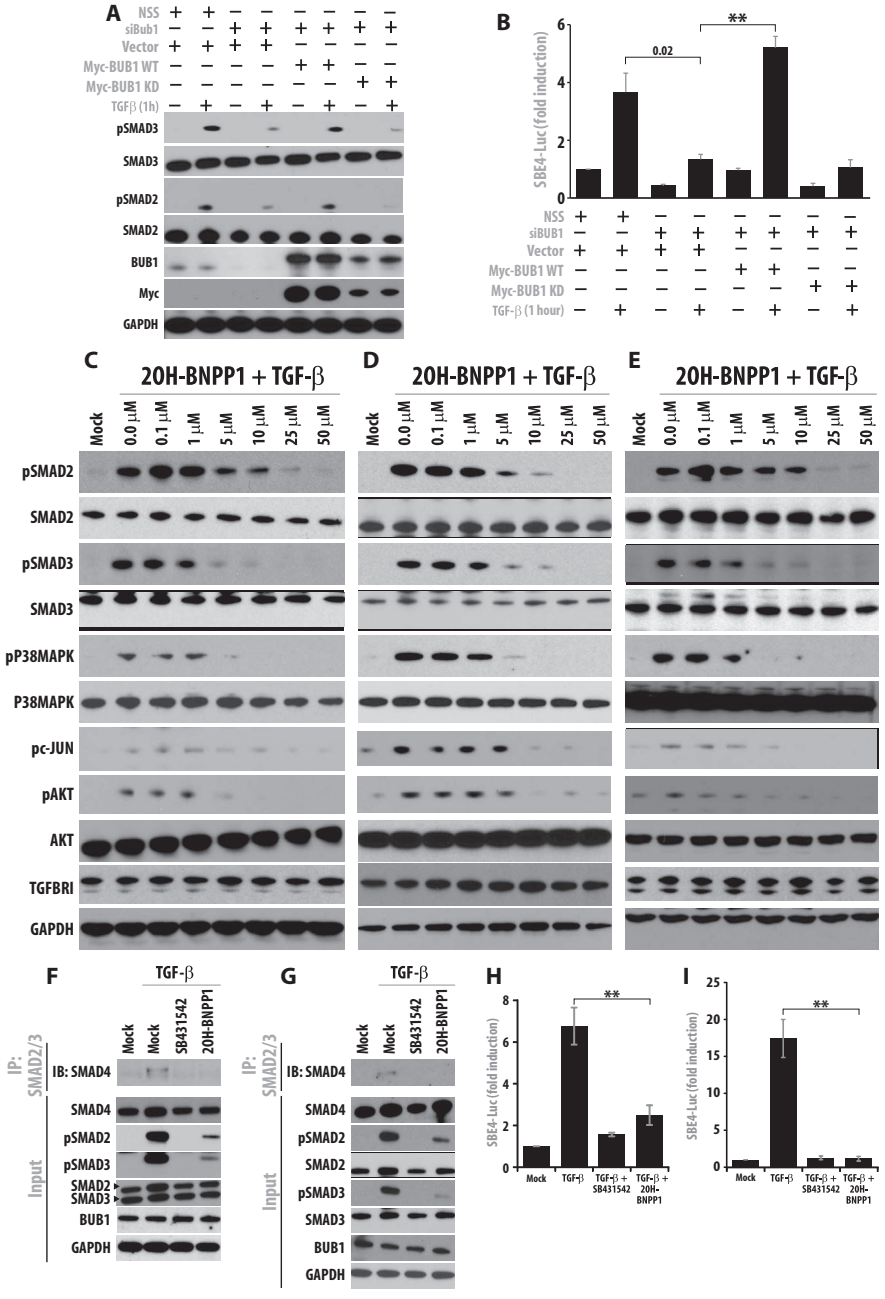


Fig. 3. BUB1 inhibitor 2OH-BNPP1 abrogates TGF-β signaling in a dose-dependent manner. (A) Immunoblotting for total and phosphorylated (p) proteins as indicated in lysates from A549 cells transiently transfected with control siRNA (NSS) or BUB1 siRNA along with wild-type BUB1 (Myc-BUB1 WT) or a kinase-deficient mutant (Myc-BUB1 KD), serum-starved, and then treated with TGF-β (10 ng/ml, 1 hour). (B) Relative luciferase activity after addition of TGF-β in A549 cell cultures described in (A) expressing the SBE4-Luc and GLuc plasmids. Data are means ± SEM of three independent experiments. (C to E) Immunoblots of lysates from A549 (C), NCI-H358 (D), and MDA-231-1833 (E) cells treated with vehicle, vehicle and TGF-β (10 ng/ml), or TGF-β and the indicated concentration of 2OH-BNPP1 for 1 hour. (F and G) IP for SMAD2/3 and then blotting for SMAD4 in lysates from A549 (F) and NCI-H358 (G) cells treated with vehicle, vehicle and TGF-β, or TGF-β and either SB431542 or 2OH-BNPP1 (10 μM) for 1 hour. (H and I) Relative luciferase activity in A549 (H) and NCI-H358 (I) cells treated as in (F) and (G) for 24 hours. Data are means ± SEM of three independent experiments. $^{**}P < 0.001$, two-sided Student's *t* test. Blots are representative of three independent experiments; blots from (C) to (E) are quantified in fig. S7.

and forms a stable receptor complex through trans-phosphorylation (*31*). To examine the role for BUB1 in the formation of this heteromeric receptor complex, A549 cells were transfected with control or BUB1-targeted siRNA and treated with TGF-β, and TGFBRI immunoprecipitates from the resulting lysates were probed for TGFBRII. BUB1 depletion abrogated the formation of the TGFBRI-TGFBRII complex (Fig. 4F). The abundance of SARA [SMAD anchor for receptor activation (*32*)] was detected in the immunoprecipitated fraction irrespective of BUB1 expression (Fig. 4F). TGF-β signaling is known to depend on the cell cycle (*33*), and BUB1 is a known regulator of the cell cycle (*8*); however, we did not observe cell cycle arrest in BUB1-depleted cells (fig. S8D).

To test whether BUB1 kinase activity played a role in the formation of the heteromeric receptor complex, we transfected A549 cells with His-tagged TGFBRI followed by treatment with 2OH-BNPP1 for 1 hour and stimulation with TGF-β for an additional hour. The TGFBRI inhibitor SB431542 was used in parallel experiments as a control. Inhibition of BUB1 kinase activity significantly reduced the formation of the TGFBRI-TGFBRII complex (Fig. 4G and fig. S9). Inhibition of BUB1 kinase activity also decreased the coimmunoprecipitation of Myc-tagged BUB1 with His-tagged TGFBRI (Fig. 4H). Because the kinase activity of BUB1 promoted the TGFBRI-TGFBRII complex formation and its own interaction with TGFBRI, we investigated whether BUB1 could directly phosphorylate TGFBRI. In vitro kinase assays revealed that BUB1 was not a direct kinase for TGFBRI (fig. S10), and although Myc-BUB1 and Flag-tagged SMAD2 coimmunoprecipitated when expressed in HEK293T cells (fig. S11), Myc-BUB1 did not phosphorylate purified SMAD3 in vitro (fig. S12). Thus, albeit important, the target of BUB1's kinase activity in the TGFBRI signaling complex was elusive.

## BUB1 interacts with TGFBRII in response to TGF-β stimulation

We next evaluated whether BUB1 also interacted with TGFBRII, which would be indicative of the formation of a ternary complex between BUB1, TGFBRI, and TGFBRII. HEK293T cells were transfected with His-TGFBRI and wild-type Myc-BUB1 and treated with 2OH-BNPP1 for 1 hour, followed by stimulation with TGF-β for an additional hour. Coimmunoprecipitation assays revealed an increase in TGF-β–stimulated interaction

Downloaded from http://stke.sciencemag.org/ on January 8, 2015

between TGFBRII and BUB1 in HEK293T cells in a kinase-dependent manner (Fig. 4I). In parallel studies, treatment of cells with the TGFBRI-specific inhibitor SB431542 did not affect this interaction (Fig. 4I).

### BUB1 inhibitor 2OH-BNPP1 abrogates SMAD2 phosphorylation in vivo

We followed up on our cellular studies by evaluating the abundance of phosphorylated SMAD2 in subcutaneous A549 tumor xenografts harvested 4 hours after mice were treated with 2OH-BNPP1. Similar to tumors from mice treated with the TGFBRI inhibitor, tumors from 2OH-BNPP1–treated mice had a significantly decreased abundance of phosphorylated SMAD2 compared with tumors from vehicle-treated mice (Fig. 5, A and B), supporting a role for BUB1 in SMAD activation.

Together, our data indicate the formation of a ternary complex between TGFBRI, TGFBRII, and BUB1, and that the kinase activity of BUB1 may promote canonical and noncanonical TGF-β signaling (Fig. 6).

## DISCUSSION

Reverse genetic screens in mammalian cells using siRNA have been used for assessing gene function, target validation, pathway analysis, gene redundancy, and therapeutic targeting of several disorders. In an effort to elucidate novel regulators of the TGF-β pathway, siRNA library screens

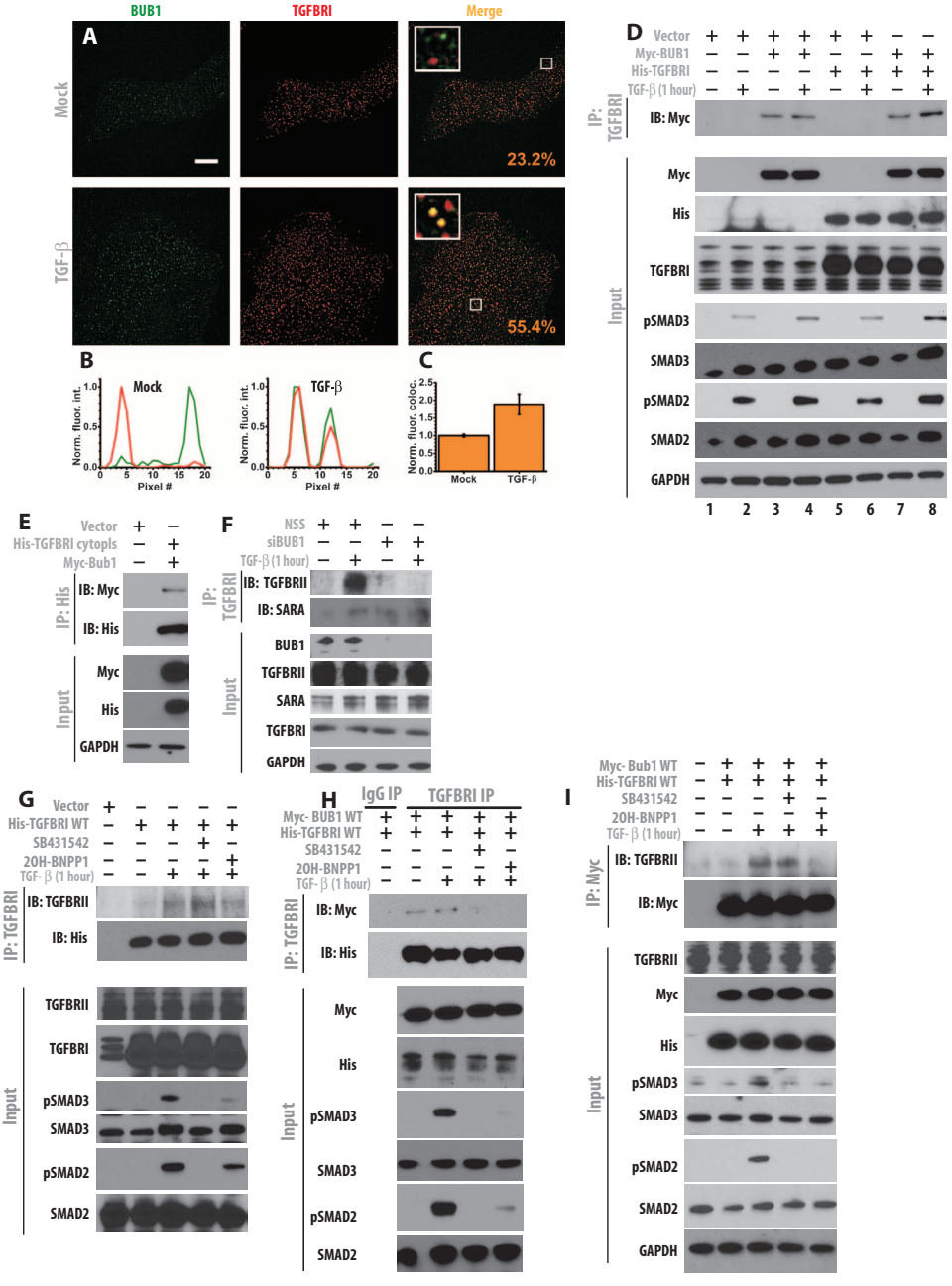


Fig. 4. BUB1 colocalizes with TGFBRI, coimmunoprecipitates with TGFBRI and TGFBRII, and promotes heteromeric TGFBRI/II complex formation. (**A**) TIRF analysis of BUB1 and TGFBRI colocalization in A549 cells treated with TGF-β (10 ng/ml) for 72 hours. Scale bar, 10 μm. (**B**) Line scan across BUB1 and TGFBRI particles within inset of (A). (**C**) Extent of colocalization normalized to the mock sample. Data are means ± SEM of three independent experiments (1000 particles, >20 cells). (**D**) IP for TGFBR1 and then blotting for Myc in lysates from A549 cells transfected with Myc-BUB1 and/or His-TGFBRI, and treated with TGF-β. 1 hour: 10 ng/ml for 1 hour. (**E**) IP for His and then blotting for Myc in lysates from A549 cells transfected with Myc-BUB1 and His-tagged cytosolic domain of TGFBRI. (**F**) IP for TGFBRI and then blotting for TGFBRII and SARA in lysates from A549 cells transfected with control or BUB1 siRNA, serum-starved, and treated with TGF-β. (**G**) IP for TGFBRI and then blotting for His and TGFBRII in lysates from A549 cells transfected with His-TGFBRI, serum-starved, and treated with SB431542 or 2OH-BNPP1 (1 hour) and then TGF-β. (**H**) IP for TGFBRI and then blotting for Myc and TGFBRII in lysates from A549 cells transfected with His-TGFBRI and Myc-BUB1, serum-starved, and treated with SB431542 or 2OH-BNPP1 (1 hour) and then TGF-β. (**I**) IP for Myc and then blotting for TGFBRII in lysates from HEK293T cells transfected with Myc-BUB1 and His-TGFBRI, serum-starved, and treated with 2OH-BNPP1 or SB431542 (10 μM, 1 hour) and then TGF-β. Blots are representative of two (I) or at least three (D to H) independent experiments.

Downloaded from http://stke.sciencemag.org/ on January 8, 2015

have identified key regulators of TGF-β signaling (*34*–*40*), although screens using TGFBRI kinase activity as a readout have not been conducted. The BTR reporter is unique in that loss of TGFBRI kinase activity results in a gain of function (increase in bioluminescence signal), and thus is less likely to result in nonspecific or off-target biological effects than are commonly observed in traditional luciferase-based screens (*4*). Recent studies using a GFP (green fluorescent protein)–fused SMAD2 reporter in a large-scale RNAi (RNA interference) screen observed that about 1% of hits exhibited off-target effects (*41*). In contrast, depletion of target genes that leads to cellular toxicity or off-target effects would be scored as false negative but not false positive when using the BTR reporter. This provided us with confidence that siRNAs that resulted in an increase in reporter activity represented true hits. A lack of overlap between hits derived from the two cell lines is not surprising considering that the physiologic response of cells to TGF-β stimulation is often cell type–and context-dependent (*42*, *43*). We focused on six hits that were common between the two cell lines, assuming that these may represent important biological regulators. Of these, BMPR2, RPS6KB1, NEK6, and JAK2 have been described to be associated with the TGF-β pathway (*44*–*48*). However, the identification of BUB1 in our siRNA screen using the TGFBRI kinase assay was surprising and unexpected due to the preponderance of literature describing BUB1 as a component of the mitotic machinery, wherein it ensures bipolar attachment to spindle microtubules so that chromatid segregation can occur with high fidelity (*7*, *8*). Confirmatory studies conducted in normal cells (MCF10A, MRC5, and Het1A) as well as tumor cell lines of various origins (A549, NCI-H358, MCF7, and MDA-231-1833) demonstrated a requirement for BUB1 expression in the cellular response to TGF-β stimulation, and thus was followed up for mechanistic studies. Additional confidence for BUB1 as a true hit was derived from studies demonstrating that depletion of BUB1 in three independent cell lines resulted in abrogation of canonical (phosphorylated SMAD2 and phosphorylated SMAD3) as well as noncanonical (phosphorylated p38 MAPK, AKT, and c-JUN) downstream effector molecules. Because TGF-β signaling has been shown to be cell cycle–dependent (*49*, *50*), we addressed the possibility that BUB1 (a regulator of mitosis) knockdown results in a decrease in TGF-β–mediated signaling due to the arrest of cells in mitosis. Existing evidence indicates that siRNA mediating complete depletion of BUB1 does not result in a cell cycle arrest (*51*), a finding confirmed in our studies (fig. S9). In addition, cell cycle dependence of TGF-β–mediated cellular responses is understood to be a downstream event wherein changes in R-SMAD phosphorylation are not altered in a cell cycle–dependent manner but are rather regulated through interaction with SKI and SNON (*5*). Last, the ability of a BUB1 kinase inhibitor to abrogate TGF-β–dependent signaling within an hour of treatment, a period during which a cell cycle arrest would not have occurred further, supports a direct role for BUB1 in receptor-mediated signaling.

The functional insights obtained in the current study suggest that BUB1 is recruited to TGFBRI in a ligand-dependent manner. Coimmunoprecipitation studies demonstrated recruitment of BUB1 to TGFBRI within an hour of TGF-β treatment, whereas TIRF microscopy demonstrated colocalization only at the 72-hour, but not earlier, time point. Superior sensitivity

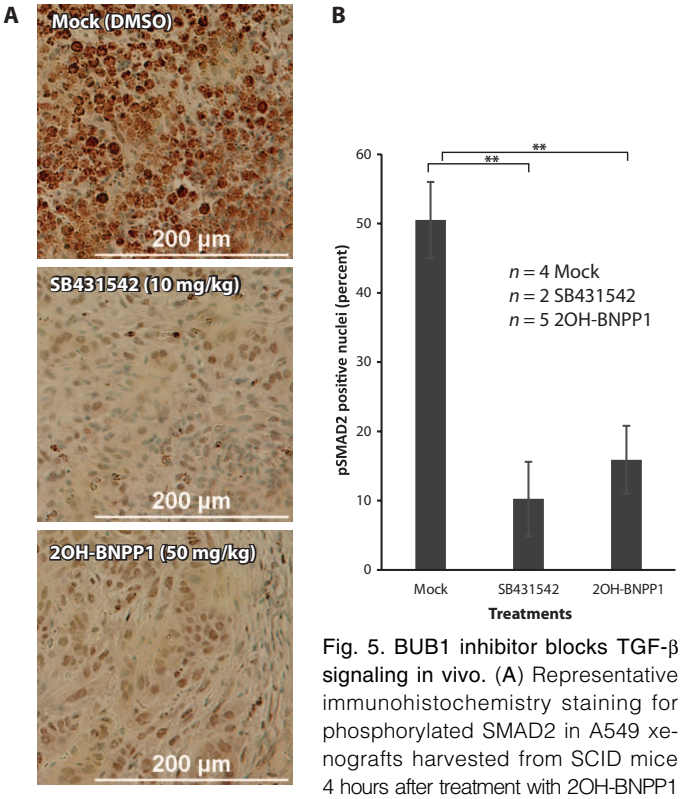


Fig. 5. BUB1 inhibitor blocks TGF-β signaling in vivo. (A) Representative immunohistochemistry staining for phosphorylated SMAD2 in A549 xenografts harvested from SCID mice 4 hours after treatment with 2OH-BNPP1 (50 mg/kg), SB431542 (10 mg/kg), or vehicle [dimethyl sulfoxide (DMSO)]. Scale bar, 200 μm. (B) Number of cells staining positive for nuclear phosphorylated SMAD2 in control ($n$ = 4), SB431542-treated ($n$ = 2), or 2OH-BNPP1–treated ($n$ = 5) mice bearing tumors. Data are means ± SEM, cell counts from three random fields for each tumor. $^{**}P < 0.001$, two-sided Student's $t$ test.

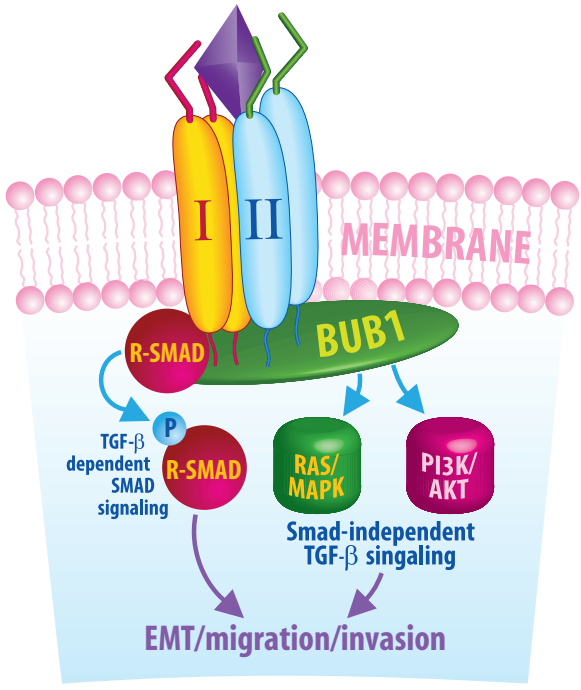


Fig. 6. A model for a role of BUB1 in TGF-β signaling. On the basis of our findings, we propose that BUB1 forms a ternary complex with TGFBRI and TGFBRII. Our data suggest that the interaction of BUB1 with TGF-β receptors is enhanced upon TGF-β stimulation, requires the kinase activity of BUB1, and promotes stabilization of the heteromeric complex between TGFBRI-TGFBRII, R-SMAD recruitment, and subsequent canonical and noncanonical TGF-β signaling cascades.

Downloaded from http://stke.sciencemag.org/ on January 8, 2015

and signal to noise of the coimmunoprecipitation experiments may explain this discordant observation. Alternatively, BUB1-TGFBRI interactions potentially occur at membrane-proximal regions, which are optically inaccessible by TIRF microscopy, at earlier time points, and these complexes are enriched at the plasma membrane only 72 hours after ligand treatment—a hypothesis that is still consistent with coimmunoprecipitation experiments that sample whole-cell lysates. Additionally, a requirement for BUB1 in the stabilization of the type II and I receptor complex, R-SMAD recruitment to the receptor, as well as co-SMAD/R-SMAD complex formation, and therefore in the downstream transcriptional response, was also demonstrated. Furthermore, our findings using a kinase dead (KD) mutant of BUB1 as well as a small-molecule inhibitor demonstrated that the kinase activity of BUB1 promotes the recruitment of BUB1 to TGFBRI and TGFBRII, as well as for TGFBRI-TGFBRII complex formation upon ligand stimulation, leading to the propagation of the cellular response to TGF-β. The biological significance of BUB1's role in TGF-β signaling was emphasized by the finding that treatment of tumor-bearing animals with 2OH-BNPP1 resulted in a loss of TGF-β–mediated SMAD2 phosphorylation to an extent similar to SB431542, an inhibitor of TGFBRI kinase activity. Our in vitro kinase assays failed to demonstrate TGFBRI or SMAD3 as direct substrates of BUB1, although we observed an interaction between BUB1 and SMAD2 in HEK293T cells. Future studies will focus on identification of substrates of BUB1 kinase activity within the TGF-β signaling pathway. Although we show that BUB1 forms a ternary complex by interacting with TGFBRI, as well as TGFBRII, the requirement for TGFBRII in the recruitment of BUB1 to TGFBRI was not directly investigated. Our studies in H358 cells, which lack TGFBRII (*52*–*54*), demonstrated a requirement of BUB1 expression and kinase activity in the propagation of the TGF-β signaling pathway, suggesting that TGFBRII may be dispensable for the interaction of BUB1 with TGFBRI.

In summary, we provide compelling evidence that BUB1 and its kinase activity are an integral component of TGF-β signaling and promote TGFBRI/II receptor complex formation, thus regulating downstream signaling cascades, including the SMAD, MAPK, and PI3K/AKT pathways. We further show that BUB1 interacts with both TGFBRI and TGFBRII and mediate TGF-β–dependent EMT, cell migration, and invasion. We anticipate that our results will lay the foundation for future studies that will provide new avenues for therapeutic targeting of TGF-β signaling in disease.

## MATERIALS AND METHODS

### Plasmid DNA

Wild-type BTR reporter has been described earlier (*4*). SBE4-Luc (*6*) reporter plasmid was provided by B. Vogelstein (Addgene plasmid #16527). pCMV5-TGFBRI-His (#19161), pCS2-Flag-SMAD2 (#14042), and pCS2-Flag-SMAD3 (#14052) were provided by J. Massague (*55*), and pCMV5B-TGFBRI-K232R (#11763) was a gift by J. Wrana (*32*). siRNA-resistant wild-type Myc-BUB1 and Myc-BUB1 KD have been previously described (*27*).

### Cell culture and transfection

The human lung carcinoma cell line A549 [American Type Culture collection (ATCC)] was maintained in RPMI 1620 medium supplemented with 10% heat-inactivated fetal bovine serum, 1% glutamine, and 0.1% penicillin/streptomycin/gentamicin (Gibco-Invitrogen). Cell cultures were grown in a humidified incubator at 37°C and 5% $CO_2$. Breast cancer cell line 1833 (*56*) derived from MDA-MB-231 was provided by J. Massague (Memorial Sloan Kettering Institute, NY) and maintained in Dulbecco's modified Eagle's medium (DMEM) in the same conditions mentioned above. NCI-H358 lung cancer cell line was provided by D. Beer (University of Michigan, Ann Arbor). Normal lung fibroblast cell line MRC5, esophageal cell line Het1A, breast epithelial line MCF7, cervical cancer cell line HeLa, and normal kidney cell line HEK293T were maintained in DMEM, whereas normal breast epithelial cell line MCF10A was maintained in special medium. All cell lines were obtained from ATCC. Cell cultures were grown in a humidified incubator at 37°C and 5% $CO_2$. A549 and MDA-231-1833 cell lines stably expressing wild-type BTR and mutant reporter were generated and maintained as described (*4*).

### Antibodies, reagents, and siRNA library

Antibodies to phosphorylated ($pSer^{465/467}$) or total SMAD2, TGFBRI, TGFBRII, $pSer^{63}$ c-JUN, $pSer^{473}$ or total AKT, $pThr^{180}/Tyr^{182}$ or total p38 MAPK, and GAPDH (glyceraldehyde-3-phosphate dehydrogenase) were all from Cell Signaling Technology. Antibody against SMAD3 was from Invitrogen; antibodies to TGFBR1 (H100) and TGFBRII (L21) were from Santa Cruz; antibodies to Myc-tag and firefly luciferase were from Millipore; antibodies to N terminus of BUB1 were from Abcam (rabbit) or Santa Cruz (goat); antibody to Flag–horseradish peroxidase (HRP) was from Sigma; and antibodies to His-HRP were from Invitrogen (clones H3 and C-term) or Millipore (H8 clone). HRP- and fluorophore-conjugated secondary antibodies were from Jackson ImmunoResearch. Recombinant human TGF-β1 was obtained from HumanZyme. TGFBRI inhibitor SB431542 was obtained from Cayman Chemical. D-Luciferin was from Xenogen Corp. The siGENOME SMARTpool siRNA library targeted against all human kinases, NSS, and individual siRNA from the siGENOME SMARTpool, and custom siRNAs against BUB1 were obtained from Dharmacon. A specific, small-molecule inhibitor of BUB1 kinase activity (2-[(4-amino-1-(*tert*-butyl)-1*H*-pyrazolo[3,4-*d*]pyrimidin-3-yl)methyl]phenol; 2OH-BNPP1) (*9*) was synthesized in-house.

### High-throughput siRNA screening against human kinases

For the high-throughput screen, A549 (5000 cells per well) and MDA-231-1833 cells (6000 cells per well) stably expressing the wild-type BTR reporter were plated in clear-bottom white-walled 96-well plates (Corning Inc.), 1 day before transfection. Twenty microliters of 2 μM of each siRNA from the siRNA kinase library was added to a V-bottom intermediate plate. Similar amount of control siRNA was also added in columns 1 and 12 in the intermediate plate (fig. S1A). The siRNAs were diluted by adding 40 μl of Opti-MEM and incubated for 5 min at room temperature. Eighty microliters of DharmaFECT 1 and Opti-MEM mix was added to the intermediate plate and incubated for an additional 30 min. All liquid handling was done using Biomek NXP Laboratory Automation Workstation (Beckman Coulter Inc.). The final assay concentration of each siRNA was 50 nM, whereas 0.2 μl of DF-1 was used for each well. Cells were incubated for 72 hours in StoreX STX44 IC precision incubator (LiCONiC Instruments), which was connected to Plate Handler II robot (PerkinElmer) and EnVision 2104 Plate Reader (PerkinElmer) with luciferin injector. TGF-β (10 ng/ml) was added to cells 1 hour before adding D-luciferin (50 μg/ml) and measuring bioluminescence. All the processes were automated. Fold change in reporter activity was calculated over change in activity in nonsilencing control siRNA (NSS)–transfected cells.

To validate hits, 100 nM siRNA to selected genes, along with TGFBRI siRNA and NSS, was transfected in A549, NCI-H358, and MDA-231-1833 cells using DharmaFECT 1. The transfected cells were incubated for 60 hours and serum-starved overnight, and TGF-β (10 ng/ml) was added 1 hour before harvesting cells for Western blotting for phosphorylated SMAD2/3, p38 MAPK, c-JUN, and AKT. Additionally, MRC5, Het1A, MCF7, and

Downloaded from http://stke.sciencemag.org/ on January 8, 2015

MCF10A cell lines were transfected in parallel experiments, and Western blotting was done to probe for phosphorylated SMAD2.

### Analysis of the siRNA screen

Data from the siRNA screen were initially analyzed on MS Excel. A quartile-based method was used for HTS (high-throughput screening) hit selection (*20*). Normalization was done with a control nontargeting siRNA (NSS) placed on each individual assay plate, and median (Q2), first (Q1), and third (Q3) quartile values were calculated for all normalized values and subjected to plate-by-plate analysis. To facilitate experiment-wide analysis, Q1, Q2, and Q3 values were calculated as described above. Averages and SE calculations were done for triplicates of log(*x*/median) values. Upper and lower boundaries were calculated as $Q3 + 2c(Q3 - Q2)$ and $Q1 - 2c(Q2 - Q1)$, respectively, for $c = 1.7239$, corresponding to a high-stringency targeted error rate ($\alpha = 0.0027$; more than 7.14-fold activation in A549 cells and more than 13.91-fold in MDA-231-1833 cells), and $c = 0.9826$, corresponding to a lower-stringency targeted error rate ($\alpha = 0.046$; more than 5.4-fold in A549 and more than 10.29-fold in MDA-231-1833 cells). High-stringency hits were chosen as those targets that scored $\alpha \leq 0.0027$ in both plate-by-plate and experiment-wide analyses. Selected targets distributed equally among all the plates, which indicates that our data did not show any "alphabetical clustering," rather agreeing on the sparse-hit hypothesis, which assumes that hits are randomly spaced throughout the data set. Selected top hits were subjected to Pathway Analysis using PathwayGuide (Advaita Corp.) to identify the pathways that are significantly affected in the BTR assay. This software uses an impact analysis that includes the classical statistics and also considers the magnitude of each gene's expression change, their type and position in the given pathways, their interaction, etc. (*57*, *58*). Two-way evidence plot, total perturbation accumulation (TA) plot, and pathway maps were generated by PathwayGuide. Functional protein association network analysis of the hits was carried out using String (http://string-db.org/). Heat maps of low- and high-stringency hits were generated using tMeV (*59*) to show data reproducibility.

### Western blot analysis

Western analysis was carried out using standard protocols. Cells were grown in culture dishes, transfected with specific siRNA, or treated with select compounds for designated time periods, and cell lysates were resolved on SDS–polyacrylamide gel electrophoresis (SDS-PAGE) gels and transferred to polyvinylidene difluoride (PVDF) membranes. Membranes were probed against specific primary antibodies followed by HRP-conjugated secondary antibodies and then visualized using the enhanced chemiluminescence (ECL) Western Blotting System (GE Healthcare). Signal intensity was measured using an image processing and analysis program (ImageJ, v1.45) (*60*).

### Coimmunoprecipitation

For coimmunoprecipitation studies, HEK293T or A549 cells were transfected with various plasmids. Lysates were made 48 hours after transfection in native lysis buffer [50 mM tris (pH 7.4), 1% NP-40, 0.25% deoxycholate sodium salt, 150 mM NaCl, 10% glycerol, and 1 mM EDTA] supplemented with 1× PhosSTOP (Roche), 1× Protease Inhibitor Cocktail (Roche), sodium orthovanadate, sodium fluoride, phenylmethylsulfonyl fluoride (PMSF), and β-glycerol phosphate (2 μM each). Cell pellet was solubilized in 600 μl of lysis buffer, rocked for 60 min at 4°C, and centrifuged at 14,000 rpm for 15 min. Protein estimation was performed with detergent-compatible DC Assay Kit (Pierce). Lysates were precleared by incubating with 50 μl of agarose beads for 1 hour at 4°C and centrifuged. Coimmunoprecipitation was carried out by incubating precleared cell lysate (400 μg of protein) with 1 to 1.5 μg of specific antibody overnight at 4°C. The immune complex was captured using 30 μl of slurry of protein A/G–coupled Sepharose beads (GE Healthcare) for 2 to 3 hours and then washed four times with lysis buffer. The resulting pellet was resolved by SDS-PAGE and transferred to PVDF membrane for Western analysis.

### SBE4-Luc reporter assay

For SBE4-Luc reporter studies, $1.25 \times 10^5$ cells (A549, NCI-H358, MDA-231-1833, and HeLa) were plated 1 day before transfection. Cells were transfected the next day with 100 ng of SBE4-Luc plasmid, 100 nM siRNA, 500 ng of various DNA, and 20 ng of Gaussia luciferase for each well with Lipofectamine 2000. Cells were serum-starved 24 hours after transfection for 6 hours and treated with TGF-β (10 ng/ml) for 24 hours (or up to 72 hours for A549) before measuring SBE4-Luc bioluminescence activity. Alternately, cells were treated with 10 μM SB431542 or 2OH-BNPP1 in the presence of TGF-β. Cells were washed twice with phosphate-buffered saline (PBS) and kept in fresh medium for 8 to 24 hours before measuring Gaussia luciferase activity. Relative firefly luciferase activity was normalized to Gaussia luciferase activity.

### Cell migration and invasion assay

Multiwell cell culture inserts (8.0-μm pore size, BD Bioscience) were used for in vitro migration assays, whereas Matrigel precoated inserts (8.0-μm pore size, BD Bioscience) were used for invasion assays. A549 cells were transfected with 100 nM siRNA, serum-starved for 6 hours with 0.5% fetal bovine serum–containing medium, treated with TGF-β (10 ng/ml) or mock for 72 hours, trypsinized, washed, and plated in serum-free medium in the inserts (25K for migration, 50K for invasion). Medium with 5% serum was added in the bottom chamber, providing a chemotactic gradient. Plates were incubated for 8 hours (migration assay) or for 24 hours (invasion assay). At the end of the assay, cells were removed from the top side of the insert using a cotton swab. Cells that penetrated to the underside surface were fixed using absolute methanol, stained with 0.5% crystal violet (Sigma), and counted under the microscope. The assay was repeated three times. The mean of three repeats run in triplicates is plotted.

### Immunofluorescence

A549 cells were plated on glass coverslips in six-well plates and transfected with 100 nM siRNA, serum-starved overnight, treated with TGF-β (10 ng/ml) for 1 hour, and processed for immunofluorescence. For the inhibitor studies, cells were plated on glass coverslips, serum-starved for 24 hours, and treated with TGF-β (10 ng/ml) in the presence of 10 μM inhibitors (SB431542 or 2OH-BNPP1) for 1 hour. Cells on coverslips were washed with PBS and fixed in 10% (v/v) buffered formalin (5 min at room temperature), followed by methanol fixation at −20°C for 20 min. Coverslips were rehydrated by incubating three times in PBS for 5 min and permeabilized in 0.2% (v/v) Triton X-100–PBS containing 1% (w/v) bovine serum albumin (BSA) on ice for 5 min. Coverslips were blocked by 5% (w/v) BSA, 5% (v/v) goat serum, and 10% (v/v) donkey serum in PBS for 1 hour. Anti-SMAD2 antibody at 1:200 dilution was added in PBS containing 0.5% (w/v) BSA and incubated for 1 hour at 37°C in a humidified chamber. Cover glasses were washed three times in PBS containing 0.025% (v/v) Triton X-100 and incubated with anti-rabbit Alexa Fluor 488 secondary antibody for 1 hour. After washing, coverslips were mounted in ProLong Gold (Invitrogen) containing DAPI (4′,6-diamidino-2-phenylindole), dried overnight at room temperature, and stored at −20°C until microscopy. Micrographs were taken using Olympus BX51 upright fluorescence microscope fitted with an Olympus DP70 high-resolution digital color camera.

### Tumor xenograft experiments and immunohistochemistry

Cell line–derived xenografts were established by implanting $2.5 \times 10^6$ A549 cells subcutaneously into each flank of 4- to 6-week-old male SCID mice.

Downloaded from http://stke.sciencemag.org/ on January 8, 2015

When tumors reached a volume between 40 and 60 $mm^3$, mice were injected with a single intraperitoneal dose of SB431542 (10 mg/kg body weight), a dose previously reported to inhibit TGF-β signaling in mouse models (*61*), 2OH-BNPP1 (50 mg/kg), or vehicle (DMSO). Tumors were excised 4 hours after treatment and fixed in formalin. Paraffin-embedded sections were stained using an antibody for phosphorylated SMAD2, and micrographs were taken with an Olympus microscope fitted with an Olympus DP70 high-resolution digital camera. The proportion of nuclei that stained positive for phosphorylated SMAD2 were counted in three random fields per tumor per treatment condition [vehicle ($n = 4$), SB431542 ($n = 2$), and 2OH-BNPP1 ($n = 5$)]. A two-sided Student's $t$ test was performed to assess statistical significance. Slides were adjusted for brightness and contrast with Adobe Photoshop CS2 (Adobe Inc.), but the micrographs underwent no further manipulations. All mouse experiments were approved by the University Committee on the Use and Care of Animals of the University of Michigan.

### Cell cycle analysis

A549 cells were plated in six-well plates and transfected with 100 nM siRNA. Cells were trypsinized 72 hours after transfection, counted, resuspended in PBS (50,000 cells/ml), fixed using 50% ethanol, stained with propidium iodide (50 μg/ml) supplemented with ribonuclease A (100 μg/ml), and read on a flow cytometer. The mean of at least three experiments is plotted.

### TIRF microscopy

A549 cells were plated on glass coverslip bottom 35-mm dishes (MatTek) and serum-starved the next day for 24 hours. Cells were treated with TGF-β (10 ng/ml) for 1, 24, or 72 hours and washed with PBS. Cells were fixed in 10% (v/v) buffered formalin for 5 min at room temperature, followed by methanol fixation at −20°C for 20 min. Cells were rehydrated by incubating three times in PBS for 5 min and were permeabilized in 0.2% (v/v) Triton X-100–PBS containing 1% BSA on ice for 5 min. Cells were blocked using 5% (w/v) BSA, 5% (v/v) goat serum, and 10% (v/v) donkey serum in PBS for 1 hour. Primary antibodies at appropriate dilution [anti-TGFBRI, 1:500; anti-BUB1 (goat), 1:35] were added in PBS containing 0.5% (w/v) BSA and incubated for 1 hour at room temperature in a humidified chamber. Plates were washed three times in PBS containing 0.025% (v/v) Triton X-100 and incubated with fluorophore-labeled secondary antibodies for 1 hour in the dark. After washing, fresh PBS was added into the plates, and TIRF microscopy was performed at the Single Molecule Analysis in Real-Time (SMART) Center using a cell-TIRF system based on an Olympus IX81 microscope, equipped with a 60× 1.49 NA (numerical aperture) oil immersion objective (Olympus). Samples were placed on a nanometer-precision motorized stage (Princeton Instruments) with *xyz* position piezo control. Images were acquired on an iXon Ultra EMCCD (electron multiplying charge-coupled device) camera (512 × 512 pixels; Andor). Alexa Fluor 488 and Alexa Fluor 647 dyes conjugated to the secondary antibodies were excited, one after another, by the 488- and 640-nm lasers, respectively. Their fluorescence was filtered through a customized quad-band filter cube consisting of a ZT405/488/561/640rpc dichroic filter (Chroma) and a ZET405/488/561/640m emission filter (Chroma). Images of BUB1 (Alexa Fluor 488) and TGFBRI (Alexa Fluor 647) were processed using a custom-compiled ImageJ macro to identify spatially distinct particles and calculate extent of colocalization.

### In vitro kinase assay

In vitro kinase assays were performed with 200 ng of protein (wild-type BUB1 or a kinase inactive mutant BUB1 KD) and 2 μg of substrate (wild-type TGFBRI, TGFBRI KD, SMAD3, or H2A) in 1× kinase buffer [50 mM tris-HCl, 150 mM NaCl, 10 mM $MgCl_2$, 1% (v/v) glycerol, 0.1% (v/v) Triton X-100, DTT (dithiothreitol), PMSF, $Na_3VO_4$ (1 mM each), 2 mM NaF, and β-glycerol phosphate] in 20-μl volume containing 10 μCi [$^{32}$P]ATP (adenosine 5′-triphosphate) and 300 μM cold ATP. Reactions were run at 30°C for 0.5 to 1 hour, quenched using Laemmli buffer, and resolved using a 4 to 12% bis-tris gel. Quantitative autoradiography was performed with a Typhoon FLA 9000 scanner (GE Healthcare).

## SUPPLEMENTARY MATERIALS

www.sciencesignaling.org/cgi/content/full/8/358/ra1/DC1

Fig. S1. siRNA screening and pathway analysis.
Fig. S2. BUB1 mediates TGF-β–dependent SMAD2/3 phosphorylation.
Fig. S3. Depletion of BUB1 leads to reduced SMAD3 recruitment to TGFBRI and TGF-β–dependent accumulation of SMAD2 in the nucleus.
Fig. S4. Depletion of BUB1 attenuates TGF-β–dependent SMAD2/3-SMAD4 complex formation in A549 cells.
Fig. S5. Depletion of BUB1 inhibits TGF-β–mediated EMT in A549 and NCI-H358 cells.
Fig. S6. Depletion of BUB1 inhibits TGF-β–mediated migration and invasion of A549 cells.
Fig. S7. BUB1 kinase activity mediates TGF-β–dependent phosphorylation and nuclear activity of R-SMAD.
Fig. S8. TGFBRI and BUB1 colocalization by TIRF microscopy at 1 and 24 hours and coimmunoprecipitation of His-TGFBRI and Myc-BUB1.
Fig. S9. BUB1 kinase activity mediates TGFBRI-TGFBRII interaction.
Fig. S10. TGFBRI is not a direct substrate of BUB1 kinase activity.
Fig. S11. Wild-type Myc-BUB1 interacts with FL-SMAD2 in HEK293T cells.
Fig. S12. SMAD3 is not a direct substrate of BUB1 kinase activity.
Table S1. Human kinome siRNA screen in A549-BTR and MDA-231-1833–BTR cells.
Table S2. Hits obtained in A549-BTR and MDA-231-1833–BTR human kinome screen.
Table S3. Pathway impact analysis based on the fold induction of the BTR reporter.

## REFERENCES AND NOTES


1. Y. Drabsch, P. ten Dijke, TGF-β signalling and its role in cancer progression and metastasis. *Cancer Metastasis Rev.* **31**, 553–568 (2012).
2. J. Xu, S. Lamouille, R. Derynck, TGF-β-induced epithelial to mesenchymal transition. *Cell Res.* **19**, 156–172 (2009).
3. R. Derynck, R. J. Akhurst, A. Balmain, TGF-β signaling in tumor suppression and cancer progression. *Nat. Genet.* **29**, 117–129 (2001).
4. S. Nyati, K. Schinske, D. Ray, M. Nyati, B. D. Ross, A. Rehemtulla, Molecular imaging of TGFβ-induced Smad2/3 phosphorylation reveals a role for receptor tyrosine kinases in modulating TGFβ signaling. *Clin. Cancer Res.* **17**, 7424–7439 (2011).
5. A. Zieba, K. Pardali, O. Söderberg, L. Lindbom, E. Nyström, A. Moustakas, C. H. Heldin, U. Landegren, Intercellular variation in signaling through the TGF-β pathway and its relation to cell density and cell cycle phase. *Mol. Cell. Proteomics* **11**, M111.013482 (2012).
6. L. Zawel, J. L. Dai, P. Buckhaults, S. B. Zhou, K. W. Kinzler, B. Vogelstein, S. E. Kern, Human Smad3 and Smad4 are sequence-specific transcription activators. *Mol. Cell* **1**, 611–617 (1998).
7. V. L. Johnson, M. I. F. Scott, S. V. Holt, D. Hussein, S. S. Taylor, Bub1 is required for kinetochore localization of BubR1, Cenp-E, Cenp-F and Mad2, and chromosome congression. *J. Cell Sci.* **117**, 1577–1589 (2004).
8. H. Yu, Z. Tang, Bub1 multitasking in mitosis. *Cell Cycle* **4**, 262–265 (2005).
9. J. S. Kang, M. J. Yang, B. Li, W. Qi, C. Zhang, K. M. Shokat, D. R. Tomchick, M. Machius, H. T. Yu, Structure and substrate recruitment of the human spindle checkpoint kinase Bub1. *Mol. Cell* **32**, 394–405 (2008).
10. S. Lawler, X. H. Feng, R. H. Chen, E. M. Maruoka, C. W. Turck, I. Griswold-Prenner, R. Derynck, The type II transforming growth factor-β receptor autophosphorylates not only on serine and threonine but also on tyrosine residues. *J. Biol. Chem.* **272**, 14850–14859 (1997).
11. S. Souchelnytskyi, P. ten Dijke, K. Miyazono, C. H. Heldin, Phosphorylation of Ser165 in TGF-beta type I receptor modulates TGF-beta1-induced cellular responses. *EMBO J.* **15**, 6231–6240 (1996).
12. A. J. Galliher, W. P. Schiemann, Src phosphorylates $Tyr^{284}$ in TGF-β type II receptor and regulates TGF-β stimulation of p38 MAPK during breast cancer cell proliferation and invasion. *Cancer Res.* **67**, 3752–3758 (2007).
13. P. Kavsak, R. K. Rasmussen, C. G. Causing, S. Bonni, H. Zhu, G. H. Thomsen, J. L. Wrana, Smad7 binds to Smurf2 to form an E3 ubiquitin ligase that targets the TGFβ receptor for degradation. *Mol. Cell* **6**, 1365–1375 (2000).
14. J. S. Kang, E. F. Saunier, R. J. Akhurst, R. Derynck, The type I TGF-β receptor is covalently modified and regulated by sumoylation. *Nat. Cell Biol.* **10**, 654–664 (2008).
15. W. Shi, C. Sun, B. He, W. Xiong, X. Shi, D. Yao, X. Cao, GADD34–PP1c recruited by Smad7 dephosphorylates TGFβ type I receptor. *J. Cell Biol.* **164**, 291–300 (2004).
16. F. Huang, Y. G. Chen, Regulation of TGF-β receptor activity. *Cell Biosci.* **2**, 9 (2012).
17. J. S. Kang, C. Liu, R. Derynck, New regulatory mechanisms of TGF-β receptor function. *Trends Cell Biol.* **19**, 385–394 (2009).
18. C. Le Roy, J. L. Wrana, Clathrin- and non-clathrin-mediated endocytic regulation of cell signalling. *Nat. Rev. Mol. Cell Biol.* **6**, 112–126 (2005).


Downloaded from http://stke.sciencemag.org/ on January 8, 2015

19. H. Mitchell, A. Choudhury, R. E. Pagano, E. B. Leof, Ligand-dependent and -independent transforming growth factor-β receptor recycling regulated by clathrin-mediated endocytosis and Rab11. *Mol. Biol. Cell* **15**, 4166–4178 (2004).
20. X. H. D. Zhang, X. T. C. Yang, N. J. Chung, A. Gates, E. Stec, P. Kunapuli, D. J. Holder, M. Ferrer, A. S. Espeseth, Robust statistical methods for hit selection in RNA interference high-throughput screening experiments. *Pharmacogenomics* **7**, 299–309 (2006).
21. M. M. Martin, J. A. Buckenberger, J. Jiang, G. E. Malana, D. L. Knoell, D. S. Feldman, T. S. Elton, TGF-β1 stimulates human $AT_1$ receptor expression in lung fibroblasts by cross talk between the Smad, p38 MAPK, JNK, and PI3K signaling pathways. *Am. J. Physiol. Lung Cell. Mol. Physiol.* **293**, L790–L799 (2007).
22. J. Y. Yi, I. Shin, C. L. Arteaga, Type I transforming growth factor β receptor binds to and activates phosphatidylinositol 3-kinase. *J. Biol. Chem.* **280**, 10870–10876 (2005).
23. J. P. Thiery, J. P. Sleeman, Complex networks orchestrate epithelial–mesenchymal transitions. *Nat. Rev. Mol. Cell Biol.* **7**, 131–142 (2006).
24. E. Meulmeester, P. Ten Dijke, The dynamic roles of TGF-β in cancer. *J. Pathol.* **223**, 205–218 (2011).
25. H. Kasai, J. T. Allen, R. M. Mason, T. Kamimura, Z. Zhang, TGF-β 1 induces human alveolar epithelial to mesenchymal cell transition (EMT). *Respir. Res.* **6**, 56 (2005).
26. J. H. Kim, Y. S. Jang, K. S. Eom, Y. I. Hwang, H. R. Kang, S. H. Jang, C. H. Kim, Y. B. Park, M. G. Lee, I. G. Hyun, K. S. Jung, D. G. Kim, Transforming growth factor β1 induces epithelial-to-mesenchymal transition of A549 cells. *J. Korean Med. Sci.* **22**, 898–904 (2007).
27. W. Qi, H. T. Yu, KEN-box-dependent degradation of the Bub1 spindle checkpoint kinase by the anaphase-promoting complex/cyclosome. *J. Biol. Chem.* **282**, 3672–3679 (2007).
28. G. J. Inman, F. J. Nicolás, J. F. Callahan, J. D. Harling, L. M. Gaster, A. D. Reith, N. J. Laping, C. S. Hill, SB-431542 is a potent and specific inhibitor of transforming growth factor-β superfamily type I activin receptor-like kinase (ALK) receptors ALK4, ALK5, and ALK7. *Mol. Pharmacol.* **62**, 65–74 (2002).
29. D. Perera, V. Tilston, J. A. Hopwood, M. Barchi, R. P. Boot-Handford, S. S. Taylor, Bub1 maintains centromeric cohesion by activation of the spindle checkpoint. *Dev. Cell* **13**, 566–579 (2007).
30. S. Pitchiaya, J. R. Androsavich, N. G. Walter, Intracellular single molecule microscopy reveals two kinetically distinct pathways for microRNA assembly. *EMBO Rep.* **13**, 709–715 (2012).
31. M. Kawabata, A. Chytil, H. L. Moses, Cloning of a novel type II serine/threonine kinase receptor through interaction with the type I transforming growth factor-β receptor. *J. Biol. Chem.* **270**, 5625–5630 (1995).
32. T. Tsukazaki, T. A. Chiang, A. F. Davison, L. Attisano, J. L. Wrana, SARA, a FYVE domain protein that recruits Smad2 to the TGFβ receptor. *Cell* **95**, 779–791 (1998).
33. Y. Wan, X. Liu, M. W. Kirschner, The anaphase-promoting complex mediates TGF-β signaling by targeting SnoN for destruction. *Mol. Cell* **8**, 1027–1039 (2001).
34. P. Cherukuri, A. J. DeCastro, A. L. Balboni, S. L. Downey, J. Y. Liu, J. A. Hutchinson, J. DiRenzo, Phosphorylation of ΔNp63α via a novel TGFβ/ALK5 signaling mechanism mediates the anti-clonogenic effects of TGFβ. *PLOS One* **7**, e50066 (2012).
35. D. J. de Gorter, M. van Dinther, O. Korchynskyi, P. ten Dijke, Biphasic effects of transforming growth factor β on bone morphogenetic protein–induced osteoblast differentiation. *J. Bone Miner. Res.* **26**, 1178–1187 (2011).
36. S. Dupont, A. Mamidi, M. Cordenonsi, M. Montagner, L. Zacchigna, M. Adorno, G. Martello, M. J. Stinchfield, S. Soligo, L. Morsut, M. Inui, S. Moro, N. Modena, F. Argenton, S. J. Newfeld, S. Piccolo, FAM/USP9x, a deubiquitinating enzyme essential for TGFβ signaling, controls Smad4 monoubiquitination. *Cell* **136**, 123–135 (2009).
37. J. Izrailit, H. K. Berman, A. Datti, J. L. Wrana, M. Reedijk, High throughput kinase inhibitor screens reveal TRB3 and MAPK-ERK/TGFβ pathways as fundamental Notch regulators in breast cancer. *Proc. Natl. Acad. Sci. U.S.A.* **110**, 1714–1719 (2013).
38. J. Mullenders, A. W. Fabius, M. M. van Dongen, H. J. Kuiken, R. L. Beijersbergen, R. Bernards, Interleukin-1R–associated kinase 2 is a novel modulator of the transforming growth factor β signaling cascade. *Mol. Cancer Res.* **8**, 592–603 (2010).
39. H. Yu, M. Königshoff, A. Jayachandran, D. Handley, W. Seeger, N. Kaminski, O. Eickelberg, Transgelin is a direct target of TGF-β/Smad3-dependent epithelial cell migration in lung fibrosis. *FASEB J.* **22**, 1778–1789 (2008).
40. L. Zhang, F. F. Zhou, Y. Drabsch, R. Gao, B. E. Snaar-Jagalska, C. Mickanin, H. Z. Huang, K. A. Sheppard, J. A. Porter, C. X. Lu, P. ten Dijke, USP4 is regulated by AKT phosphorylation and directly deubiquitylates TGF-β type I receptor. *Nat. Cell Biol.* **14**, 717–726 (2012).
41. N. Schultz, D. R. Marenstein, D. A. De Angelis, W. Q. Wang, S. Nelander, A. Jacobsen, D. S. Marks, J. Massagué, C. Sander, Off-target effects dominate a large-scale RNAi screen for modulators of the TGF-β pathway and reveal microRNA regulation of *TGFBR2*. *Silence* **2**, 3 (2011).
42. H. Ikushima, K. Miyazono, Cellular context-dependent "colors" of transforming growth factor-β signaling. *Cancer Sci.* **101**, 306–312 (2010).
43. S. S. Söderberg, G. Karlsson, S. Karlsson, Complex and context dependent regulation of hematopoiesis by TGF-β superfamily signaling. *Ann. N. Y. Acad. Sci.* **1176**, 55–69 (2009).
44. C. Petritsch, H. Beug, A. Balmain, M. Oft, TGF-β inhibits p70 S6 kinase via protein phosphatase 2A to induce $G_1$ arrest. *Genes Dev.* **14**, 3093–3101 (2000).
45. P. ten Dijke, H. Yamashita, H. Ichijo, P. Franzén, M. Laiho, K. Miyazono, C. H. Heldin, Characterization of type I receptors for transforming growth factor-beta and activin. *Science* **264**, 101–104 (1994).
46. M. Barrios-Rodiles, K. R. Brown, B. Ozdamar, R. Bose, Z. Liu, R. S. Donovan, F. Shinjo, Y. M. Liu, J. Dembowy, I. W. Taylor, V. Luga, N. Przulj, M. Robinson, H. Suzuki, Y. Hayashizaki, I. Jurisica, J. L. Wrana, High-throughput mapping of a dynamic signaling network in mammalian cells. *Science* **307**, 1621–1625 (2005).
47. C. Dees, M. Tomcik, K. Palumbo, A. Akhmetshina, A. Horn, P. Zerr, O. Distler, G. Schett, J. H. W. Distler, JAK2 mediates the stimulatory effects of transforming growth factor beta on fibroblast activation and tissue fibrosis. *Arthritis Rheum.* **63**, S944–S945 (2011).
48. X. Wang, S. Shaw, F. Amiri, D. C. Eaton, M. B. Marrero, Inhibition of the Jak/STAT signaling pathway prevents the high glucose-induced increase in TGF-β and fibronectin synthesis in mesangial cells. *Diabetes* **51**, 3505–3509 (2002).
49. J. Song, EMT or apoptosis: A decision for TGF-β. *Cell Res.* **17**, 289–290 (2007).
50. T. Hirschhorn, L. Barizilay, N. I. Smorodinsky, M. Ehrlich, Differential regulation of Smad3 and of the type II transforming growth factor-β receptor in mitosis: Implications for signaling. *PLOS One* **7**, e43459 (2012).
51. P. Meraldi, P. K. Sorger, A dual role for Bub1 in the spindle checkpoint and chromosome congression. *EMBO J.* **24**, 1621–1633 (2005).
52. T. K. Kim, E. K. Mo, C. G. Yoo, C. T. Lee, S. K. Han, Y. S. Shim, Y. W. Kim, Alteration of cell growth and morphology by overexpression of transforming growth factor β type II receptor in human lung adenocarcinoma cells. *Lung Cancer* **31**, 181–191 (2001).
53. W. S. Kim, C. Park, Y. S. Jung, H. S. Kim, J. Han, C. H. Park, K. Kim, J. Kim, Y. M. Shim, K. Park, Reduced transforming growth factor-beta type II receptor (TGF-beta RII) expression in adenocarcinoma of the lung. *Anticancer Res.* **19**, 301–306 (1999).
54. Y. Shintani, M. Maeda, N. Chaika, K. R. Johnson, M. J. Wheelock, Collagen I promotes epithelial-to-mesenchymal transition in lung cancer cells via transforming growth factor-β signaling. *Am. J. Respir. Cell Mol. Biol.* **38**, 95–104 (2008).
55. A. Hata, R. S. Lo, D. Wotton, G. Lagna, J. Massagué, Mutations increasing autoinhibition inactivate tumour suppressors Smad2 and Smad4. *Nature* **388**, 82–87 (1997).
56. Y. B. Kang, P. M. Siegel, W. P. Shu, M. Drobnjak, S. M. Kakonen, C. Cordón-Cardo, T. A. Guise, J. Massagué, A multigenic program mediating breast cancer metastasis to bone. *Cancer Cell* **3**, 537–549 (2003).
57. S. Draghici, P. Khatri, A. L. Tarca, K. Amin, A. Done, C. Voichita, C. Georgescu, R. Romero, A systems biology approach for pathway level analysis. *Genome Res.* **17**, 1537–1545 (2007).
58. A. L. Tarca, S. Draghici, P. Khatri, S. S. Hassan, P. Mittal, J. S. Kim, C. J. Kim, J. P. Kusanovic, R. Romero, A novel signaling pathway impact analysis. *Bioinformatics* **25**, 75–82 (2009).
59. A. I. Saeed, V. Sharov, J. White, J. Li, W. Liang, N. Bhagabati, J. Braisted, M. Klapa, T. Currier, M. Thiagarajan, A. Sturn, M. Snuffin, A. Rezantsev, D. Popov, A. Ryltsov, E. Kostukovich, I. Borisovsky, Z. Liu, A. Vinsavich, V. Trush, J. Quackenbush, TM4: A free, open-source system for microarray data management and analysis. *Biotechniques* **34**, 374–378 (2003).
60. M. D. Abramoff, P. J. Magalhães, S. J. Ram, Image processing with ImageJ. *Biophotonics Int.* **11**, 36–42 (2004).
61. Y. Chen, C. S. Kam, F. Q. Liu, Y. Liu, V. C. Lui, J. R. Lamb, P. K. Tam, LPS-induced upregulation of TGF-β receptor 1 is associated with TNF-α expression in human monocyte-derived macrophages. *J. Leukoc. Biol.* **83**, 1165–1173 (2008).


**Acknowledgments:** We thank S. Kronenberg for help in figure graphics, and T. Cunningham with preparation of the manuscript. We also thank the Microscopy & Image Analysis Laboratory and the DNA Sequencing Core at the University of Michigan Medical School. **Funding:** This work was supported by grants from the NIH: P01CA85878, P50CA093990, and R01CA136892 (B.D.R. and A.R.), P50CA093990-11 (Career Development Award; S.N.), as well as NSF MRI-R2-ID award DBI-0959823 (N.G.W.). **Author contributions:** S.N., B.D.R., and A.R. conceived and designed the study and wrote the manuscript with input from all the authors. S.N. performed most of the experiments. K.S.-S. assisted in the high-throughput screen. S.P. performed TIRF microscopy analysis. K.C., A.C., N.C., and J.D. provided experiment support. M.E.V.D. synthesized the 2OH-BNPP1 inhibitor. S.V. and C.K.-S. assisted, and N.G.W., M.K.N., and D.R. analyzed the HTS data. H.Y. provided reagents, contributed to the experimental design, and assisted in the interpretation of results. **Competing interests:** The authors declare that they have no competing interests. **Data and materials availability:** Data for the kinome siRNA screen are deposited in PubChem (https://pubchem.ncbi.nlm.nih.gov/assay/assay.cgi?aid=1117269), accession ID 1117269. Materials may be requested from the corresponding author. There is a patent pending for the use of targeting BUB1 therapeutically.

Submitted 14 April 2014
Accepted 7 November 2014
Final Publication 6 January 2015
10.1126/scisignal.2005379
**Citation:** S. Nyati, K. Schinske-Sebolt, S. Pitchiaya, K. Chekhovskiy, A. Chator, N. Chaudhry, J. Dosch, M. E. Van Dort, S. Varambally, C. Kumar-Sinha, M. K. Nyati, D. Ray, N. G. Walter, H. Yu, B. D. Ross, A. Rehemtulla, The kinase activity of the Ser/Thr kinase BUB1 promotes TGF-β signaling. *Sci. Signal.* **8**, ra1 (2015).

Downloaded from http://stke.sciencemag.org/ on January 8, 2015

Science Signaling
AAAS

**The kinase activity of the Ser/Thr kinase BUB1 promotes TGF-β signaling**

Shyam Nyati, Katrina Schinske-Sebolt, Sethuramasundaram Pitchiaya, Katerina Chekhovskiy, Areeb Chator, Nauman Chaudhry, Joseph Dosch, Marcian E. Van Dort, Sooryanarayana Varambally, Chandan Kumar-Sinha, Mukesh Kumar Nyati, Dipankar Ray, Nils G. Walter, Hongtao Yu, Brian Dale Ross and Alnawaz Rehemtulla

(January 6, 2015)
*Science Signaling* **8** (358), ra1. [doi: 10.1126/scisignal.2005379]

The following resources related to this article are available online at http://stke.sciencemag.org. This information is current as of January 8, 2015.

**Article Tools** Visit the online version of this article to access the personalization and article tools:
http://stke.sciencemag.org/content/8/358/ra1

**Supplemental Materials** *"Supplementary Materials"*
http://stke.sciencemag.org/content/suppl/2015/01/02/8.358.ra1.DC1.html

**Related Content** The editors suggest related resources on *Science*'s sites:
http://stke.sciencemag.org/content/sigtrans/7/344/re8.full.html
http://stke.sciencemag.org/content/sigtrans/3/119/tr4.full.html
http://stke.sciencemag.org/content/sigtrans/7/345/ra91.full.html
http://stke.sciencemag.org/content/sigtrans/7/335/rs5.full.html
http://stke.sciencemag.org/content/sigtrans/7/345/eg3.full.html
http://stke.sciencemag.org/content/sigtrans/1/46/eg8.full.html
http://stke.sciencemag.org/cgi/cm/stkecm;CMN_9915
http://stke.sciencemag.org/cgi/cm/stkecm;CMP_9876

**References** This article cites 61 articles, 24 of which you can access for free at:
http://stke.sciencemag.org/content/8/358/ra1#BIBL

**Glossary** Look up definitions for abbreviations and terms found in this article:
http://stke.sciencemag.org/cgi/glossarylookup

**Permissions** Obtain information about reproducing this article:
http://www.sciencemag.org/about/permissions.dtl

*Science Signaling* (ISSN 1937-9145) is published weekly, except the last December, by the American Association for the Advancement of Science, 1200 New York Avenue, NW, Washington, DC 20005. Copyright 2015 by the American Association for the Advancement of Science; all rights reserved.

Downloaded from http://stke.sciencemag.org/ on January 8, 2015